Z-CONTRAST SCANNING TRANSMISSION ELECTRON MICROSCOPY AS A TOOL FOR INTERFACE ANALYSIS IN NANOCRYSTAL-POLYMER NANOCOMPOSITES.

A.V. KADAVANICH†*, T. KIPPENY*, M. ERWIN*, S. J. ROSENTHAL*, S. J. PENNYCOOK†
†Oak Ridge National Laboratory, Solid State Division, Oak Ridge, TN 37831,
*Vanderbilt University, Department of Chemistry, Nashville, TN 37235

ABSTRACT

We have applied Atomic Number Contrast Scanning Transmission Electron Microscopy (Z-Contrast STEM) towards the study of colloidal CdSe semiconductor nanocrystals embedded in MEH-PPV polymer films as used for a prototype photovoltaic device.

Atomic resolution imaging reveals both the lateral shape and thickness profile of nanocrystals embedded in the film.

Electron Energy Loss Spectroscopy (EELS) at sub-nanometer resolution was used to investigate the chemical composition at the nanocrystal polymer interface. We find evidence for oxygen aggregation at the interface, consistent with at maximum one monolayer of surface oxide on the nanocrystals.

INTRODUCTION

CdSe nanocrystals are under investigation for heterojunction optoelectronic devices, such as light-emitting devices (LED's) and photovoltaics (PV's).[1-3] The performance of such devices should be very sensitive to the nature of the junction interface which is the interface between the nanocrystal and the surrounding matrix, usually a conducting polymer. Despite many studies, nanocrystal surfaces are not very well understood in detail since bulk techniques average over all the different surfaces on a nanocrystal and scanning probes do not penetrate the organic ligands on the surface.

In this paper we present the use of a high resolution Scanning Transmission Electron Microscope (STEM) to obtain information about the individual surfaces on a nanocrystal. In particular using a high-angle annular dark-field (HAADF) detector provides Z-Contrast which can resolve the sublattice in CdSe nanocrystals. Hence the polarity of the unit cell can be assigned directly from the Z-Contrast image without resorting to extensive image simulations. Furthermore, since the Z-Contrast image is a direct projection of the atomic positions, the technique is sensitive to aperiodic detail at the surface unlike phase-contrast HRTEM.[4,5]

Using the sub-nanometer STEM probe for EELS analysis allows chemical analysis on the length scale of a few Å. In principle it should thus be possible to obtain both chemical and structural information from individual nanocrystal surfaces in the STEM.[6]

EXPERIMENT

Sample Preparation

CdSe nanocrystals were prepared by the method of Murray[7,8] as modified by Peng[9] for size-focussing. The TOPO surface ligands were exchanged with pyridine by heating in anhydrous pyridine for several hours. The nanocrystals were subsequently precipitated with hexanes and dissolved in chloroform. Poly (2-methoxy,5-(2'-ethyl-hexyloxy)-p-phenylenevinylene) (MEH-PPV) was prepared by the method of Wudl[10] and dissolved in chloroform. CdSe samples were stored in a glovebox until use, MEH-PPV was stored under argon in brown glass vials. TEM samples were prepared by mixing the MEH-PPV and CdSe solutions and spin-coating onto single-crystal NaCl substrates (100 surfaces). Typical parameters were 20μl of 2 mg•ml^{-1} MEH-PPV/0.05 mg•ml^{-1} CdSe solution, spun at 2000 rpm. The films were removed by dipping into a water surface, whereupon the film floats onto the surface as the NaCl dissolves away. The floating films were picked up with lacey carbon coated copper TEM grids (Ted Pella Co.). Film thicknesses were typically in the range from 150-200 Å as judged from the optical absorption of identical films spun onto glass slides. Attempts to directly measure the film thickness using AFM have so far not yielded reliable results but indicate significant roughness on the order of 50Å consistent with ellipsometry measurements. Specimens for EELS analysis were prepared in a glovebag (Aldrich Atmosbag) purged with dry nitrogen and stored under nitrogen or argon. Specimens were loaded with a glovebag attached to the microscope

under nitrogen flow (unfiltered, from a standard gas cylinder). Specimens for Z-contrast imaging were prepared in air, stored under argon, and loaded in air.

STEM

EELS analysis was performed in a Vacuum Generators (VG) model HB501 STEM operating at 100kV with an ultimate resolution of 2.2Å. However, to improve the signal-to-noise ratio (SNR) for EELS data collection, the probe was run with low excitation of the condenser lens and the exact probe size was not measured. A parallel EELS system using a CCD detector with near single-electron sensitivity was employed. The system is described in more detail in [6]. Data were analyzed using Wavemetrics Igor Pro 3.13. Pre-edge backgrounds were fitted to a power law function and subtracted. Integration of stripped edges used Igor Pro's algorithm based on the trapezoidal method.

To obtain EELS line profiles, an image was taken before and after scanning and scans with excessive image drift (more than ~10Å) were rejected. The actual linescan is obtained by scanning the probe at a constant rate across the specimen in the x-direction only. EELS spectra are acquired successively at fixed signal integration times resulting in a series of EELS measurements at different points along the line.

Z-Contrast imaging was performed in a VG HB603 STEM operating at 300kV with a nominal resolution of 1.3Å. Raw images were deconvoluted using a Maximum Entropy [11-13] algorithm running on a dedicated PC with a custom coprocessor card. The details are described elsewhere.[4] For presentation, image brightness/contrast was adjusted in NIH Image 1.61.

For a single atom, the image contrast is proportional to the square of the atomic number (Z^2). For a crystalline specimen in a channeling orientation, the intensity also depends on the thickness of an atomic column along the beam direction. The dependence is non-linear but monotonic and can be calculated from the known crystal structure for any given channeling direction. For typical nanocrystal sizes (<80Å) the dependence is nearly linear so that intensities can be used for comparing relative thicknesses between atomic columns. Intensities are measured in NIH Image by manually selecting a region around each column, summing the values of all pixels in the chosen region and subtracting the value of the background near the column.

RESULTS/DISCUSSION

EELS

EELS spectra are collected in the range from 500 eV to 950 eV. The pre-edge background for each EELS spectrum is fit to a power law function and subtracted to obtain the Oxygen K-edge signal at 532 eV. Edge intensities are integrated in the range from 532 eV to 600 eV To obtain the linescan shown in Figure 1, the probe was scanned immediately after acquiring the image. Another image was obtained after the scan to gauge specimen drift. Spectra were collected in seventeen 4 second increments while continuously scanning the probe along the line indicated in the figure. The total drift in the image for the entire linescan was about 10Å, predominantly to the right, so that the positional uncertainty in each step is less than 1 Å. The edge intensities indicate the relative oxygen content as a function of position along the scan.

The depletion of oxygen at the center of the nanocrystal is due to the

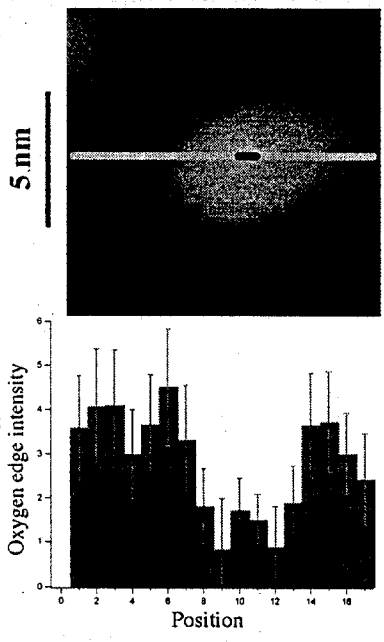

Fig. 1:
Top: DF image of a single nanocrystal with the linescan indicated by the horizontal line. The marker in the center indicates the length of each scan step and thus the area integrated for each EELS measurement.
Bottom:
The oxygen concentration profile calculated from the EELS oxygen K-edge intensity at each scan step. The depletion at the center is attributed to the excluded volume of MEH-PPV.

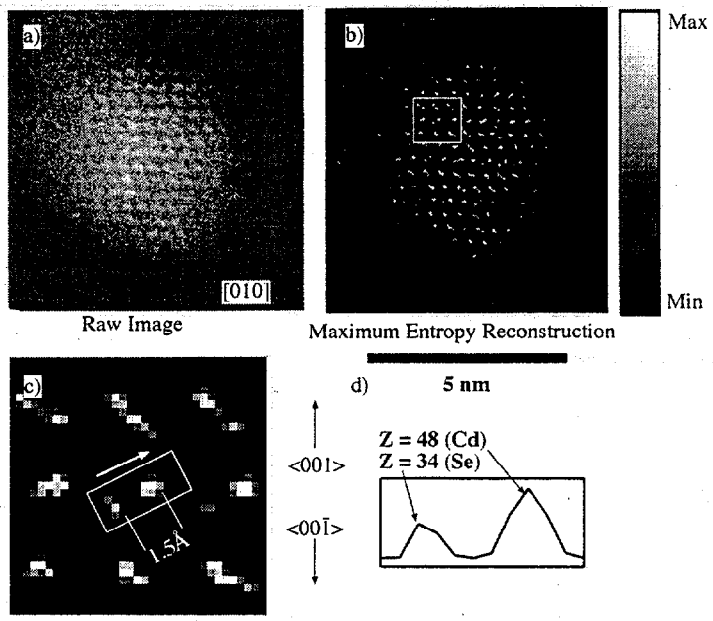

Fig. 2:
a) Z-STEM image of a CdSe nanocrystal near [010] zone axis orientation.
b) Maximum Entropy Reconstruction of the object function
c) enlarged view of the area delimited by the box in (b). The dumbbell pairs can be resolved into the atomic columns 1.5 Å apart.
d) line scan in the direction of the arrow in (c) showing the intensity in the two columns. The intensity distribution closely matches the expected contrast for Cd relative to Se (2:1). Hence the directions of the <001> and <00-1> lattice vectors can be assigned to the image as shown.

exclusion of MEH-PPV. The slight increase at the edges of the nanocrystal is suggestive of a thin oxide shell viewed in projection, but within the measurement uncertainty it is not significant. Hence no firm conclusion can be drawn although it does demonstrate the potential for surface specific chemical analysis. It should be noted that the acquisition parameters correspond to detecting less than 10 atoms of oxygen within a scan increment on the MEH-PPV.

Z-STEM

The Z-STEM image of a nanocrystal near [010] zone axis orientation is shown in Figure 2. Panel (a) shows the raw image and panel (b) is the Maximum Entropy (MaxEnt) Reconstruction of the object function with the point spread function of the microscope removed. Panel (c) shows a magnified view of the area in (b) indicated by the square. The dumbbell pairs of Cd and Se columns spaced 1.5Å apart are just resolved. The different intensities indicate that the Cd comprises the top right column of the dumbbell pair. This is more evident from the integrated intensity profile in (d) of the area indicated. Based on the contrast in the atomic column the <001> lattice vector direction is assigned as up in the image.

Not all columns are as well resolved within this image. This could indicate strain in the lattice, but it could also be due to image noise. The maximum SNR in the raw image is approximately 2. While the atomic centers are well separated (1.5Å) the actual object function is not a delta function. Rather the scattering potential corresponds to 1s Bloch states centered on the atomic positions. These states have a diameter on the order of 0.8Å so some overlap between the Se and Cd states may be expected. The low SNR then makes it very difficult to accurately resolve the dumbbells. In fact, in one case, the intensity ratio is reversed, with the Se position showing higher intensity than the Cd position and an intensity ratio of 0.8. However, the remaining measurements (13 other dumbbells could be adequately resolved) all support the assignment of the <001> direction

It is assumed that the Cd and Se columns are of equal thickness within each dumbbell column. One may reasonably expect them to differ by one atom at the entrance and exit surfaces each, depending on the exact nature of the surface termination. For the nanocrystal shown the thickness should be on the order of 15-18 atoms so the maximum error would be 13% which cannot account for the contrast difference observed. Hence the assignment of the elemental identities is clear-cut.

If we integrate the total intensity of each dumbbell pair we obtain a spatially resolved thickness map, since the intensities are then independent of composition. This analysis is shown in Figure 3. The thickness envelope corresponds to the expected shape based on previous HRTEM studies on such nanocrystals. [14] However, in this case the three-dimensional information is obtained in concert with the 2-dimensional projection, directly from the image.

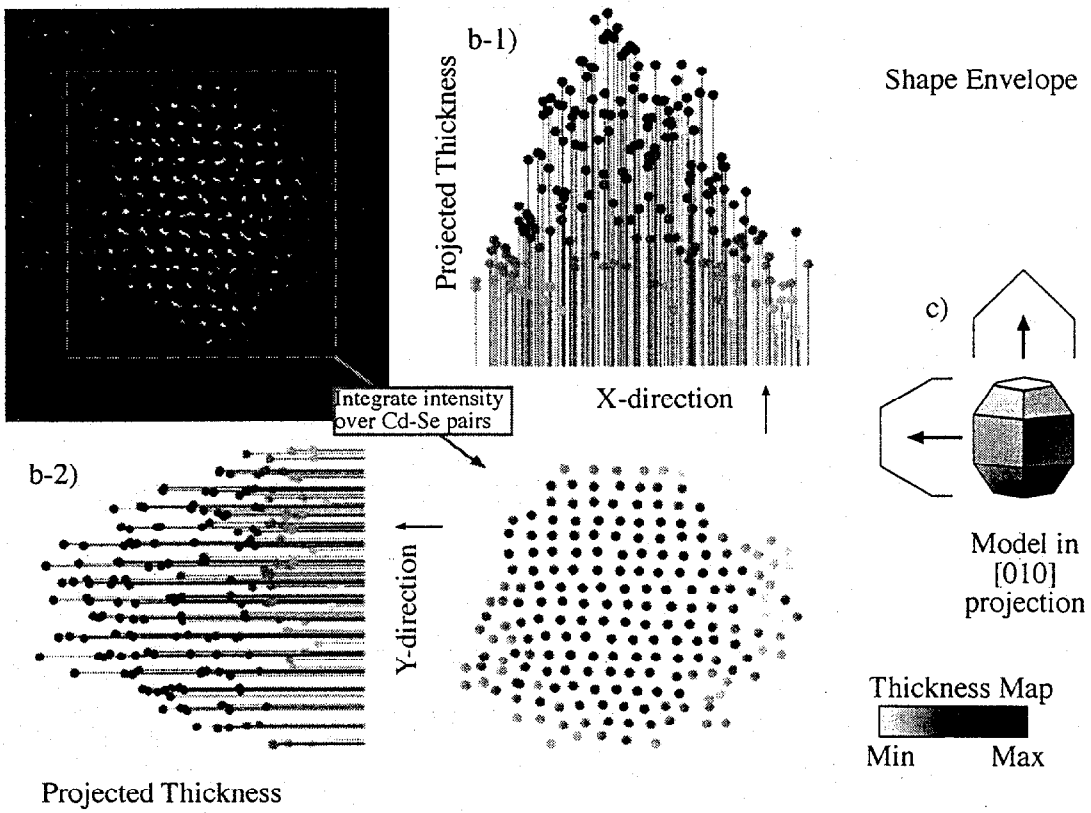

Fig. 3: 3-D Analysis of CdSe nanocrystal
a) the Z-STEM image after Maximum Entropy Reconstruction
b) Thickness map (raw intensity) on a grayscale after integrating the intensity in each dumbbell pair (or otherwise resolvable feature in the image). The indicated thickness is not corrected for the thickness dependence of the contrast, so values are not absolute.
b-1) Projection of the thickness map along the horizontal direction in the image. The envelope of the thicknesses should correspond to the shape envelope of the nanocrystal.
b-2) Same as b-1) in the vertical direction.
c) Schematic of the expected shape in [010] projection based on previous HRTEM studies and the expected shape envelopes in each projection.

The low SNR also makes it difficult to accurately identify the positions of surface atom columns. Additionally, the MaxEnt does a poor job at fitting the flat background signal from the polymer, giving rise to spurious features in the region surrounding the particle. The Pixon™ method, a more recent image reconstruction algorithm [15-17] avoids this overfitting resulting in the smoother image shown in Figure 4. In addition to the smoother background, the image more accurately reflects the spatial extent of the Bloch states giving rise to the image. Overall the information obtained is the same as that from the MaxEnt reconstruction of Fig. 2, except for the surface region which appears much less ambiguous. This is the first time the Pixon™ method has been applied to Z-STEM data so further testing will be necessary to ensure that the results can stand up to scrutiny. Nevertheless the early results are promising.

CONCLUSIONS

Using sub-nanometer STEM probes it is possible to obtain chemical information on individual nanocrystals from spatially resolved EELS measurements. Linescans across CdSe nanocrystals suggest a surface oxide layer but the assignment is ambiguous at present.

Z-Contrast STEM is capable of resolving the lattice polarity in CdSe nanocrystals and can also provide thickness information directly from the image. Surface detail should be resolvable but the currently available data is not of sufficient quality yet.

FUTURE WORK

The EELS linescans would be easier to interpret if the polymer matrix did not contribute to the oxygen signal. To that end we are currently testing the use of poly-3-hexylthiophene (P3HT) as the polymer matrix. Any oxygen then detected could be unambiguously assigned to the nanocrystals.

The Analysis of the Z-STEM data is crucially reliant on obtaining good SNR. In the short term this requires optimizing the specimen preparation to reduce drift and beam damage, allowing longer signal averaging. Presently, beam damage is the limiting factor as the MEH-PPV seems to degrade under the electron beam and cause contamination buildup. It remains to be seen if P3HT will perform better in this regard.

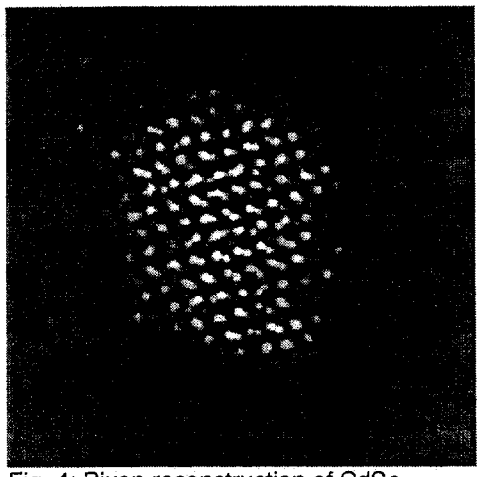

Fig. 4: Pixon reconstruction of CdSe nanocrystal

In the long term the installation of a spherical aberration corrector will result in a beam profile with vastly improved imaging characteristics. The resolution will be improved to 0.5Å and the SNR is expected to improve by a factor of 7. The corrector will also reduce tailing in the beam profile, which makes it feasible to attempt column-resolved EELS measurements. The corrector is currently scheduled to be operational in early 2002 and should radically improve the capabilities of Z-STEM microanalysis.

ACKNOWLEDGEMENTS

The research presented here was funded by the Department of Energy, Basic Energy Sciences, Materials Sciences Division.

We wish to thank R. Puetter for performing the pixon reconstruction shown. We also wish to thank A. Yahil and Pixon LLC for a research use licence to the commercial Pixon™ code.

AVK gratefully acknowledges the assistance of P.D. Nellist, B.E. Rafferty, M. F. Chisholm, Y. Yan and G. Duscher in the operation of the STEM and EELS systems. We wish to thank C. Chen and G. Jellison for ellipsometry and J. Taylor for AFM measurements on films.

REFERENCES

1. Schlamp, M.C., Peng, X. & Alivisatos, A.P. *Journal of Applied Physics* **82**, 5837-42 (1997).
2. Colvin, V.L., Schlamp, M.C. & Alivisatos, A.P. *Nature* **370**, 354-357 (1994).
3. Greenham, N.C., Xiaogang, P. & Alivisatos, A.P. *Physical Review B (Condensed Matter)* **54**, 17628-37 (1996).
4. Pennycook, S.J., Jesson, D.E., McGibbon, A.J. & Nellist, P.D. *Journal of Electron Microscopy* **45**, 36-43 (1996).
5. Nellist, P.D. & Pennycook, S.J. *Journal of Microscopy-Oxford* , 159-170 (1998).
6. Duscher, G., Browning, N.D. & Pennycook, S.J. *Physica Status Solidi A* **166**, 327-42 (1998).
7. Murray, C.B., Norris, D.J. & Bawendi, M.G. *Journal Of the American Chemical Society* **115**, 8706-8715 (1993).
8. Bowen Katari, J.E., Colvin, V.L. & Alivisatos, A.P. *Journal of Physical Chemistry* **98**, 4109-17 (1994).
9. Peng, X.G., Wickham, J. & Alivisatos, A.P. *Journal Of the American Chemical Society* **120**, 5343-5344 (1998).
10. Wudl, F. & Srdanov, G. in *United States Patent* (United States of America, 1993).
11. Burch, S.F., Gull, S.F. & Skilling, J. *Computer Vision, Graphics, and Image Processing* **23**, 113-28 (1983).

12. Skilling, J. & Bryan, R.K. *Monthly Notices of the Royal Astronomical Society* **211**, 111-24 (1984).
13. Skilling, J. & Sibisi, S. in *Invited and Contributed Papers from the Conference* (ed. Johnson, M.W.) 1-21 (IOP, Chilton, UK, 1990).
14. Shiang, J.J., Kadavanich, A.V., Grubbs, R.K. & Alivisatos, A.P. *Journal of Physical Chemistry* **99**, 17417-17422 (1995).
15. Puetter, R.C. *International Journal of Imaging Systems and Technology* **6**, 314-331 (1995).
16. Pina, R.K. & Puetter, R.C. *Publications of the Astronomical Society of the Pacific* **105**, 630-637 (1993).
17. Pina, R.K. & Puetter, R.C. *Publications of the Astronomical Society of the Pacific* **104**, 1096-1103 (1992).